EFFICIENT LOCOMOTION ON NON-WHEELED SNAKE-LIKE ROBOTS

Julián Colorado, Antonio Barrientos, Claudio Rossi, Mario Garzón, María Galán, Jaime del Cerro
Robotics and Cybernetics Group, Robotics and Automation Center UPM-CSIC, Universidad Politécnica de Madrid, Spain
jcolorado@etsii.upm.es, antonio.barrientos@upm.es, claudio.rossi@upm.es, j.cerro@upm.es

Keywords: Serpenoid curves, Snake bio-mechanisms, Bio-inspired locomotion, Crawling robots.

Abstract: This article presents our current work on studying energy efficient locomotion on crawling snake-like robots. The aim of this work is to use existing biological inspired methods to demonstrate lateral undulation planar gaits for efficiently controlling high-speed motion as a function of the terrain surface. A multilink non-wheeled snake-like robot is being developed for experimentation and analysis of efficient serpentine locomotion based on simulation results.

1 INTRODUCTION

In nature, snakes are able to move on different environments. Generally speaking, snakes can adapt to a particular terrain employing changes in their muscles-shape (Kane and Lecision, 2000). This potential provides snakes with higher rough terrain adaptability on irregular surfaces compared to legged animals.

The first attempts of approaching biological inspired snake motion using an artificial counterpart was conducted by Hirose in the 70's (Hirose, 1993). He made the analysis of limbless motions experimental data and suggested mathematical description of the snake's instant form. The curve was called –*serpenoid*– and is widely used for the snake robot's control assignment nowadays. The first designs of Hirose's snake robots had modules with small passive wheels, and since then, most of the current developments (Downling, 1997), (Chirikjian and Burdick, 1990), (Ostrowski, 1995) remain using snake robots with wheels in order to facilitate forward propulsion. Nonetheless, snake-like robots that have no wheels are closer to their biological counterparts. The difficulty in analyzing and synthesizing snake locomotion mechanisms is not as simple as wheeled mechanisms. One of the main drawbacks relies on their poor power efficiency for surface traction, and consequently locomotion. While most works address contributions in terms of snake control and full autonomous navigation (Kamegawa et al., 2002), (Prautsch and Mita, 1996), (Transeth et al., 2006) our work is focused on providing modeling foundations to use a non-wheeled snake robot that can adapt to the environment at the advantage of energy efficiency.

Our goal is to establish a mathematical framework for modeling that relates the existing knowledge of biological snake locomotion with the dynamics behavior that achieves minimal energy waste when the snake moves at high speeds over 1m/s. Section 2 of this article briefly presents how to achieve lateral undulation serpentine gaits using Hirose's serpenoid curves and how to integrate that approach within the dynamics equations of motion. A friction model is also addressed in order to achieve the proper forward motion based on internal joint torques. Section 3 introduces how to optimize snake locomotion by choosing the optimal serpenoid curve parameters that minimize energy consumption. Simulation results show efficient motion over ground. Finally, Section 4 presents conclusions and upcoming future work will present experimental validation using an experimental testbed (under current development) that consists on nine articulated modules serially connected.

2 SERPENTINE MODELING

Almost all limbless vertebrates, including snakes, mimic their ancestors by shaping their bodies in a

–*S-shaped*– curve that travels tailwards (Gray and Lissmann, 1950). Snakes commonly propel themselves on the ground or water by summing the longitudinal resultants of lateral forces. This kind of motion is called *Lateral Undulation* (see Figure 1).

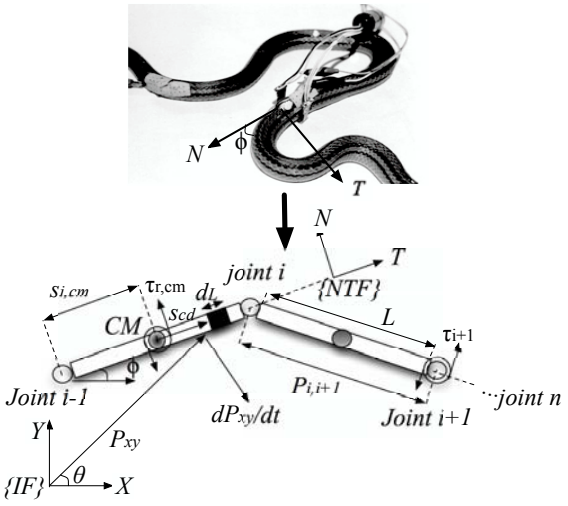

Figure 1: (Above): The *s-shape* that biological snakes perform to move forward using lateral undulation pattern. (Below): serially coupled rigid body system description.

Table I introduces a description of the variables involved within the framework of snake-like robot modeling based on Figure 1.

TABLE I
DESCRIPTION OF SNAKE-LIKE ROBOT PARAMETERS

Description	Notation	Units
Number of links	n	-
Joint position at body-*i*	ϕ_i	[rad]
Body-*i* orientation with respect to inertial frame {IF}	θ_i	[rad]
Vector position from joint's frame to body's CM	$\vec{s}_{i,cm}$	[m]
Distance from body's CM to differential length d_L	s_{cd}	[m]
Link-*i* length	L	[m]
Vector position from joint-*i* frame to joint *i+1*	$\vec{p}_{i\,i+1}$	[m]
Joint torque of body-*i*	τ_i	[Nm]
Friction torque of body-*i* CM	$\tau_{r,cm}$	[Nm]
Friction coefficients	C_N, C_T	[s^{-1}]

2.1 Serpenoid curves

Hirose found that snakes take their body onto so-called serpenoid curve when they move with a serpentine gait. Considerer the snake-like robot depicted in Figure 1, which consist on *n*-links serially connected through *n-1* joints. The undulatory motion of a snake can be imitated by changing the relative angles ϕ of snake's bodies as shown in Equation 1. See details in (Hirose and Morishima, 1990).

$$\phi_i(t) = 2\alpha \sin\left(\omega_s t + (i-1)\beta\right) + \gamma \qquad (1)$$

The term $\phi_i(t)$ is a sinusoidal function varying along the arc length i/n $\left(\forall_i : i = 1...n-1\right)$ at ω_s angular speed propagation. The terms, α, β and γ are the parameters that determine the shape of the serpentine curve realized by the snake-like robot (e.g. if $\gamma = 0$, the curve will describe a straight path and when $\gamma \neq 0$ the curve will trace a circular path). Equation 2 shows these parameters.

$$\alpha = a\left|\sin\left(\frac{\beta}{2}\right)\right|, \quad \beta = \frac{b}{n}, \quad \gamma = -\frac{c}{n} \qquad (2)$$

Based on different choices of the parameters a, b and c, Figure 2 shows several serpenoid curves profiles. The parameter a determines the degree undulation, b the number of periods in a unit length, and c is the motion circular bias.

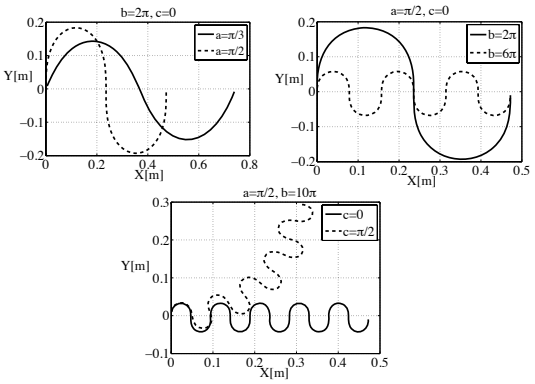

Figure 2: Computing Lateral Undulation serpentine gaits using serpenoid curves.

Our first objective is to merge this serpentine curve approach into our snake dynamics model. The key property of snakes in achieving forward locomotion is the difference in the friction coefficients for the tangential–*T* and the normal–*N* directions with respect to the body. In particular, the normal friction tends to be much larger than the tangential friction, leading to avoidance of side slipping. In order to analyze such property, next subsection introduces the solution of the dynamic's Equations of Motion –EoM of a multilink articulated

body system as shown in Figure 1, and the incorporation of a simple friction model to provide accurate snake forward propulsion.

2.2 Snake-like robot dynamics

Applying the D'Alembert's principle (Fu et al., 1987) and assuming a snake's tail (base) to end-body (head) recursive propagation of kinematics spatial velocities in (3) [angular and linear components stacked in a single 6-dimensional quantity]:

$$V_i = P_{i-1,i}^T R_{i,i-1}^T V_{i-1} + H_i \dot{\phi}_i \quad \{\forall_i : i = 1...n\} \tag{3}$$

In multibody dynamics, spatial quantities must be propagated and projected onto unique frames in order to be operator on. For this purpose, operators for translation: $P_{i-1,i} \in \Re^{6x6}$ and rotation: $R_{i,i-1} \in \Re^{6x6}$ are defined as:

$$P_{i-1,i} = \begin{bmatrix} I & \tilde{p}_{i-1,i} \\ 0 & I \end{bmatrix}, \quad R_{i,i-1} = \begin{bmatrix} r_{i,i-1} & 0 \\ 0 & r_{i,i-1} \end{bmatrix}, \tag{4}$$

where $I \in \Re^{3x3}$ is the identity operator, $\tilde{p}_{i-1,i} \in \Re^{3x3}$ is the skew symmetric matrix corresponding to the vector cross product of $\vec{p}_{i-1,i} \in \Re^3$, which is any vector joining e.g. joint *i* to joint *i+1* in Figure 1. The term $r_{i,i-1} \in \Re^{3x3}$ refers to the generalized rotation matrix that takes any point in coordinate frame-*i* and projects it onto frame *i-1*. The joint velocity $\dot{\phi}_i$ is obtained by taking the derivative of Equation (1) with respect to time (serpenoid curve). Finally the $H_i \in \Re^6$ vector allows the projection of the joint velocity with respect to the axis of motion of the joint.

Differentiating Equation (3) with respect to time, the spatial accelerations are:

$$\begin{aligned} \dot{V}_i = {} & P_{i-1,i}^T R_{i,i-1}^T \dot{V}_{i-1} + H_i \ddot{\phi}_i + \dot{P}_{i-1,i}^T R_{i,i-1}^T V_{i-1} \\ & + \dot{H}_i \dot{\phi}_i \quad \{\forall_i : i = 1...n\}, \end{aligned} \tag{5}$$

where the third and fourth terms corresponds to coriolis and centrifugal accelerations. Finally, a backward propagation of spatial forces yields:

$$\begin{aligned} F_i = {} & J_i \dot{V}_i + \left[\dot{J}_i - \dot{S}_{i,cm} J_i\right] V_i + R_{i,i-1} P_{i-1,i} F_{i+1} \\ & + S_{i,cm} F_{ri,cm} \quad \{\forall_i : i = n...1\}, \end{aligned} \tag{6}$$

where $J_i \in \Re^{6x6}$ is the mass operator defined by the inertia tensor. The operator $S_{i,cm} \in \Re^{6x6}$ has the same structure of $P_{i-1,i} \in \Re^{6x6}$ in Equation (4), and corresponds to the distance ($\vec{s}_{i,cm} \in \Re^3$) between the joint frame and the CM of the body. Finally the joint toques are: $\tau_i = H_i^T F_i$.

2.3 Modeling surface friction

Friction force is essential to achieve forward motion. From Equation (6), the term $F_{ri,cm} \in \Re^6$ is the friction force referred to the CM frame and yields:

$$F_{ri,cm} = \begin{bmatrix} 0 & 0 & \tau_{r,cm} & f_{r,xi} & f_{r,yi} & 0 \end{bmatrix}^T, \tag{7}$$

where $\tau_{r,cm}$ is the torque friction component due to planar rotation, and the terms $\left[f_{r,xi}, f_{r,yi}\right]$ are the components due to translation. Differentiating the position vector P_{xy} with respect to time:

$$P_{xy} = \begin{bmatrix} X \\ Y \end{bmatrix} + \begin{bmatrix} c\theta \\ s\theta \end{bmatrix} s_{cd}, \quad \dot{P}_{xy} = \begin{bmatrix} \dot{X} \\ \dot{Y} \end{bmatrix} + \begin{bmatrix} -s\theta \\ c\theta \end{bmatrix} s_{cd}\dot{\theta} \tag{8}$$

Modeling the linear friction for the differential d_L with respect to the {NTF}-frame yields:

$$\begin{bmatrix} df_{r,T} \\ df_{r,N} \end{bmatrix} = -\begin{bmatrix} C_T & 0 \\ 0 & C_N \end{bmatrix} \begin{bmatrix} \tilde{v}_T \\ \tilde{v}_N \end{bmatrix} dm_i \tag{9}$$

Considering that the tangential and normal velocity $\left[\tilde{v}_T, \tilde{v}_N\right]$ are related to the linear velocity $\dot{P}_{xy}$ with the following transformation:

$$\begin{bmatrix} \tilde{v}_T \\ \tilde{v}_N \end{bmatrix} = \begin{bmatrix} c_\theta & s_\theta \\ -s_\theta & c_\theta \end{bmatrix} \begin{bmatrix} \dot{X} \\ \dot{Y} \end{bmatrix}, \tag{10}$$

the translation friction force is:

$$\begin{bmatrix} f_{r,xi} \\ f_{r,yi} \end{bmatrix} = -m \begin{bmatrix} c_\theta^2 C_T - s_\theta^2 C_N & s_\theta c_\theta \left(C_T - C_N\right) \\ s_\theta c_\theta \left(C_T - C_N\right) & s_\theta^2 C_T + c_\theta^2 C_N \end{bmatrix} V_i \tag{11}$$

The C_T and C_N parameters are the tangential and normal coefficients. In addition, the component of the total friction torque for the differential d_L is:

$$\begin{aligned} \tau_{r,cm} &= -C_N \int s_{cd} \left(\tilde{v}_N + s_{cd}\dot{\theta}\right) dm \\ &= -C_N \left(\int s_{cd} \tilde{v}_N dm + \int s_{cd}^2 \dot{\theta} dm \right) \end{aligned} \tag{12}$$

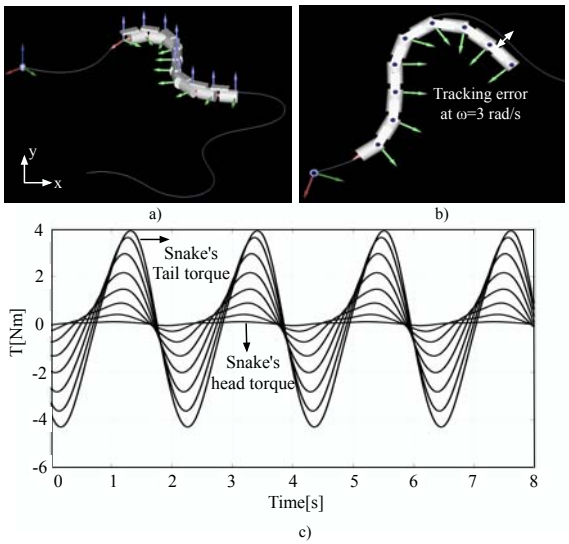

Figure 3: Snake-like robot simulation: a). Circular serpenoid curve using $\gamma = 1.2^{\circ}$, b). *Top view* tracking error due to inefficient friction and serpenoid parameters tuning, c). Joint torques to move the snake forward.

Assuming the relation: $dm = m \cdot L^{-1} ds$ (being L the length of a body-*i*; see Figure 1), the friction torque about the body-*i* CM is:

$$\tau_{r,cm} = -C_N \frac{m}{L} \dot{\theta} \int_0^L s_{cd}^2 \, ds = -\frac{C_N m L^2}{3} \dot{\theta} \tag{13}$$

Using Equations (11) and (13), the total friction force vector denoted by Equation (7) is incorporated into the dynamic's EoM of the snake-like robot (see Equation (6)).

Once the snake modelling is completed, Figure 3 depicts the 8-degree of freedom snake-like robot (*n=8*) performing a circular serpenoid trajectory profile: $\alpha = 0.5 rad$, $\beta = 1.1 rad$, $\omega_s = 2.5 rad/s$.

Friction coefficients make the robot to generate larger friction forces in the normal direction than in the tangential direction of the motion. Considering $C_T = 12$, $C_N = 20$ and the mass of each snake's link in $m = 0.4 kg$. Despite the snake is capable of propelling forward, a tracking error (caused by external friction forces) appears when the snake is speeding up. These preliminary results suggest us to analyze how to relate energy consumption (input power against speed), and how to tune friction parameters as a function of that speed and serpenoid curve terms. For this purpose, our goal in the next section is to find how to change the serpenoid curve parameters in Equation (2) to achieve the energy-efficient locomotion based on the dynamic's EoM in Equation (6).

3 EFFICIENT SNAKE MOTION

Friction force represents a power loss. Part of the input power generated by the snake's actuators is converted into kinetic energy K_E and the rest is lost due to the friction.

The objective of this section is to find the optimally efficient motion within the dynamics framework of serpentine locomotion. More precisely, our challenge is related to choosing the parameters α, β, ω_s that make the average power loss P_L in Equation (14) minimal while keeping a prescribed average speed.

$$P_L = m V_i^T \begin{bmatrix} -C_N m L^2 / 3 & 0 \\ 0 & 0 \end{bmatrix} \cdot \begin{bmatrix} c_\theta^2 C_T - s_\theta^2 C_N & s_\theta c_\theta (C_T - C_N) \\ s_\theta c_\theta (C_T - C_N) & s_\theta^2 C_T + c_\theta^2 C_N \end{bmatrix} V_i \tag{14}$$

The approach we used is to increase the speed of the snake and verifying where is the saturation point that preserves an efficient locomotion in terms of power loss compared to the total energy of the system described in Equation (15) as:

$$K_E = \sum_{i=1}^{n} \frac{1}{2} \dot{\phi}_i^T J(\phi) \dot{\phi}_i . \tag{15}$$

The first set of tests consists on varying the serpenoid curve parameters described in Equation (2). Considering angular speeds from $\omega_s = [0...4]$, we have analyzed the relationship between input energy and speed. Results are shown in Figure 4.

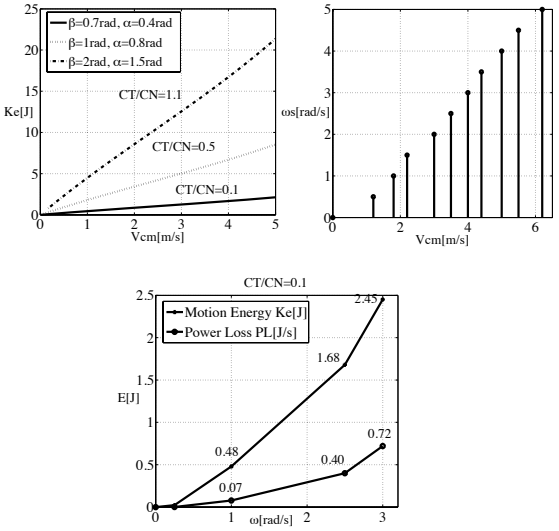

Figure 4: Energy and velocity relationship for different average of serpenoid curve profiles α, β, ω_s for *n*=8.

Two preliminary important considerations can be made. First of all, the relation to maintain between friction coefficients as a function of the snake morphology for *n*=8 (i.e. size, weight, mass distribution), and the serpenoid curve profile (i.e. undulation degree of the curve, speed, direction) is about $C_T/C_N = 0.1$. This friction ratio has been found from taking the simulation-results average for what choices of the serpenoid parameters α, β, ω_s the percentage of power loss is minimal. In this case, at maximum serpentine speed angular propagation of $\omega_s = 3rad/s$, we achieved a maximum power loss about 30%. Increasing the ratio of friction coefficients under the same characteristics, the energy consumption also increases and consequently performance was compromised. Note that these friction ratios strictly depend on the snake's dynamics and the terrain characteristics. For experimental testing, we will have to explore and test different kind of materials that achieve the proper friction ratio dependent of different surfaces of motion. Using this relation, the snake is capable to move forward wasting the minimum energy and achieving the required velocity; in other words, this is the optimal relation between serpenoid curve parameters, snake morphology, and friction forces. In addition, also note in Figure 4 that using this optimal relationship, the snake linear velocity V_{cm} and the serpenoid curve speed ω_s are roughly proportional to each other.

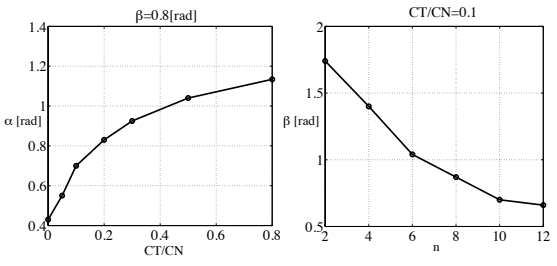

Figure 5: Serpenoid curve phase β and undulation degree α as a function of friction coefficients C_T/C_N and the snake's number of links *n*.

The tests performed in Figure 4, allowed us to find the optimal energy relation between:

- Energy consumption K_E and P_L.
- Velocity V_{cm} and ω_s.
- Friction C_T/C_N and parameters β and α.

Nonetheless note from Equation 2 that β and α are also strictly dependent on the snake configuration, this means, the snake number of links: *n*.

Thus, we have carried out a second series of tests varying the number of links (*n*) of the snake and changing the terrain surface, i.e., changing ratios of C_T/C_N. From the results depicted in Figure 5, we found that α is affected as a function of friction modification, whereas β depends on the number of links-*n*. Regarding the same simulation scenario in Figure 3 (circular snake motion using $\gamma = 1.2^\circ$), this time we use optimal relationships to achieve energy-efficient and reliable snake locomotion. The optimal parameters configuration is: $\alpha = 0.7rad, \beta = 0.8rad$, $n = 8, C_T = 1, C_N = 10, \omega_s = 3rad/s$.

Figure 6 illustrates the simulation results for open-loop tracking of the circular serpenoid path.

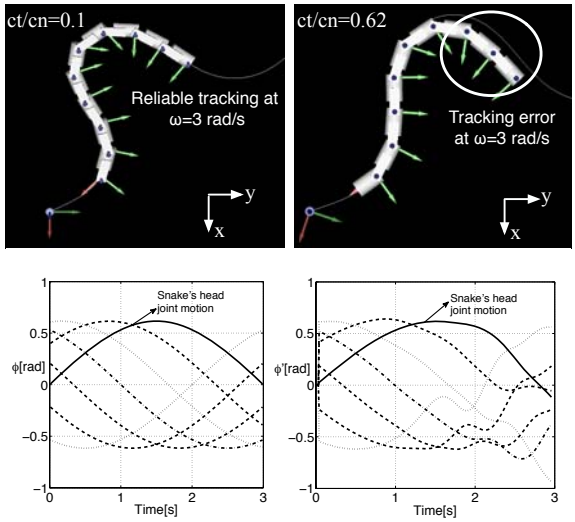

Figure 6: Cartesian (above) and Joint positions (below) between efficient snake locomotion (left) against improper parameters tuning (right), at snake speed of $\omega_s = 3rad/s$.

The simulation scenario shown in Figure 3 is now compared to the efficient approach of serpentine locomotion showed in Figure 6. The joint position error ϕ' (inefficient approach) is about 12.5% against 2.2% for the efficient approach (ϕ). Table II consigns several simulations on testing efficient snake locomotion for different speed profiles.

TABLE II
EFFICIENCY OF SERPENOID LOCOMOTION FOR $C_T/C_N = 0.1$

	Test-1	**Test-2**	**Test-3**	**Test-4**
ω_s [rad/s]	0.25	1.04	2.5	3
%error ϕ	0.59%	0.98%	1.15%	2.2%
K_E[J]	0.022	0.48	1.68	2.45
P_L [J/s]	$9.2x10^{-4}$	0.077	0.40	0.72
% P_L	4.11%	5.75%	23.80%	29.38%
Efficiency	0.95	0.83	0.76	0.70

4 CONCLUSIONS AND FUTURE WORK

The dynamics framework for the modelling and simulation of non-wheeled snake-like robots has been presented. Bio-inspired kinematics locomotion was efficiently integrated into our approach of achieving efficient serpentine locomotion at high-speeds. Simulation results depicted in Table II showed that our first hypothesis was indeed correct. Considering speeds up to 4 m/s we obtained efficient motion (less than 30%) of power loss due to friction. For speeds >4m/s, this efficiency decreases because of the increase of the angular speed, which also makes the friction force increases and subsequently generating more power loss average that makes the control effort too energetic. This speed boundary was obtained from several simulations performed in Figures 4 and 5. In conclusion, the key aspects in regarding energy efficient serpentine locomotion are basically synthesized as: 1). α is an increasing function of C_T/C_N, thus, the snake robot should undulate with larger amplitude when the friction ratio is larger (i.e. the snake-like robot tends to slip in the normal direction), 2). ω_s is basically a liner function of the linear speed V_{cm}, and, 3). β is a decreasing function of *n*.

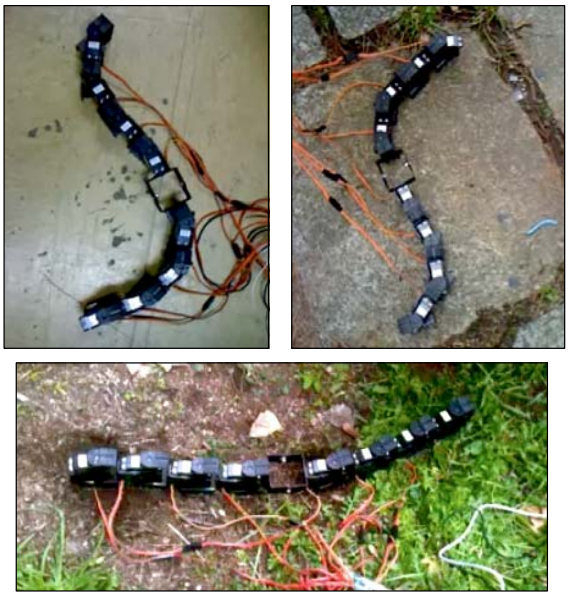

Figure 7: Locomotion testing experiments over different friction terrains.

These relationships are useful for determining the optimal control law for the snake robot. Upcoming work is oriented towards the full implementation of the hardware/software that allow the snake robot to be fully controlled. Using a first prototype depicted in Figure 7, our current work is focused on researching which materials and shapes of the snake's skeleton generate the proper friction and traction using our modeling approach.

ACKNOWLEDGEMENTS

This work is funded by the project ROBOCITY 2030 (S2009/DPI-1559).

REFERENCES

Chirikjian, G.S., and Burdick, J.W., 1990. An obstacle avoidance algorithm for hyper-redundant manipulators. *In IEEE International Conference on Robotics and Automation*, pag. 625–631, Cincinnati.

Dowling, K.J., 1997. Limbless Locomotion: Learning to Crawl with a Snake Robot. *PhD thesis, Carnegie Melon University*, Pittsburgh, USA.

Fu, K.S., Gonzalez, R.C., and Lee C.S.G., 1987. *Robotics: Control, Sensing, Vision, and Intelligence*. New York:McGraw-Hill.

Gray, J., and Lissmann, H., 1950. The kinetics of locomotion of the grass-snake, *J. Exp. Biol.*, vol. 26, no. 4, pp. 354-367.

Hirose, S., 1993. Biologically inspired robots (snake-like locomotor and manipulator). *In Oxford University Press.*

Hirose, S., and Morishima, A., 1990. Design and control of a mobile robot with an articulated body, *Int. J. Robot. Res.*, vol. 9, no. 2, pp. 99-114.

Kane, T., and Lecison, D., 2000. Locomotion of snakes: A mechanical 'explanation', *Int. J. Solids Struct.*, vol. 37, no. 41, pp. 5829–5837.

Kamegawa, T., Matsuno, F., and Chatterjee, R., 2002. Proposition of Twisting Mode of Locomotion and GA based Motion Planning for Transition of Locomotion Modes of a 3-dimensional Snake-like Robot, *Proc. IEEE Int. Conf. on Robotics and Automation*, pp. 1507

Ostrowski, J., 1995. The Mechanics of Control of Undulatory Robotic Locomotion. *PhD thesis, California Institute of Technology*.

Prautsch, P., and Mita, T., 1999. Control and Analysis of the Gait of Snake Robots. *Proceedings of the IEEE International Conference on Control Applications*, Kohala Coast-Island of Hawaii, Hawaii, USA, pp. 502.

Transeth, A., and Pettersen, K.Y., 2006. Developments in snake robot modeling and locomotion, in *Proc. IEEE Int. Conf. Control, Automation, Robotics and Vision*, pp. 1393–1400.